

# Disentangling the Assembly History of Galaxies and Super-Massive Black Holes with 21-cm Observations from the Lunar Farside

Jordan Mirocha  
NLSI Forum 07.17.2012

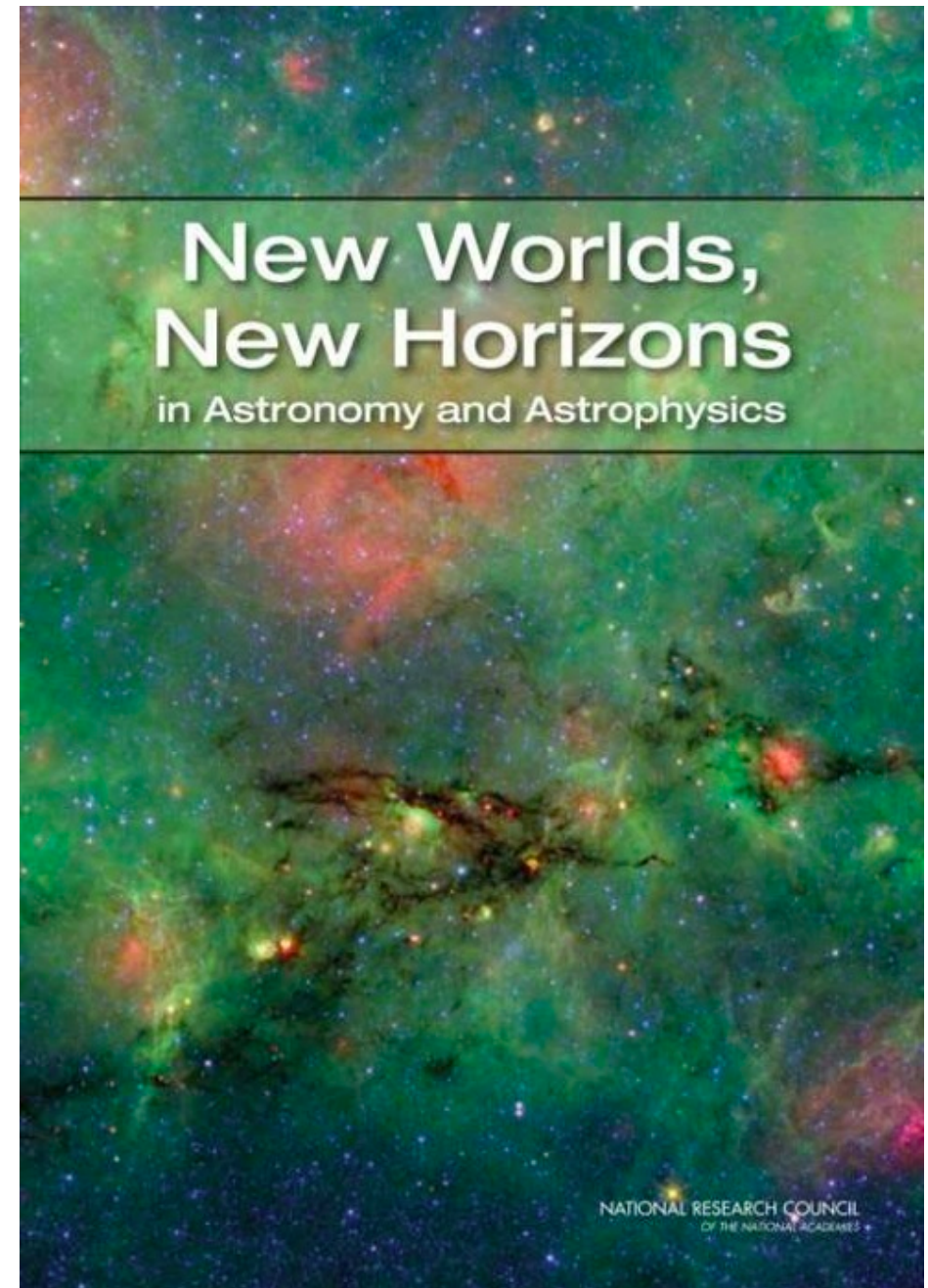
Collaborators: Jack Burns, Stephen Skory, Geraint Harker,  
Abhi Datta, John Wise, Steven Furlanetto

# Outline

- Big picture questions
- The global 21-cm background
- X-rays from accreting black holes

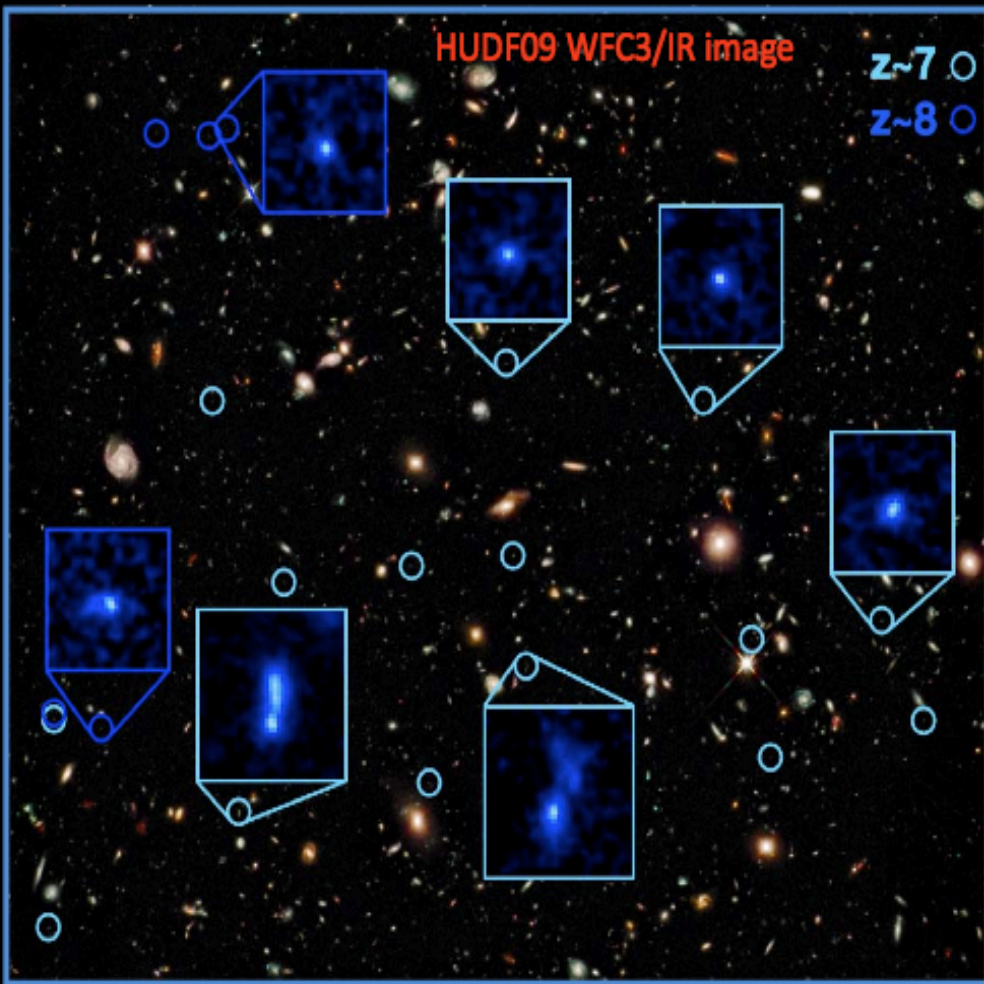
# Big picture

- When did the first stars, galaxies, and black holes form?
- What were their properties?
- When was reionization complete, and what objects drove it?



# Galaxy Formation

Hubble is pushed to the limit to find these galaxies



HUDF09 WFC3/IR image

z~7

z~8

examples of the 16 redshift  $z \sim 7$  sources and 5  $z \sim 8$  galaxies we found in the HUDF with the WFC3/IR and the ACS.  
(Bouwens et al and Oesch et al papers)

these galaxies are seen just 600-800 million years from the big bang

very competitive arena: three other teams have reported similar results at  $z \sim 7-8$  (Bunker et al; McLure et al; Yan et al)

galaxies in the first 700 million years Garth Illingworth [www.firstgalaxies.org](http://www.firstgalaxies.org) [gdi@ucolick.org](mailto:gdi@ucolick.org)

- Galaxies at  $z \sim 7$  are 1/20 the size and  $< 1\%$  the mass of the Milky Way
- Extremely blue
- Metal deficient

Image Credit: Garth Illingworth

# Black Holes

Mortlock et al. 2011



- Quasar at  $z = 7.085$
- 770 million years after Big Bang

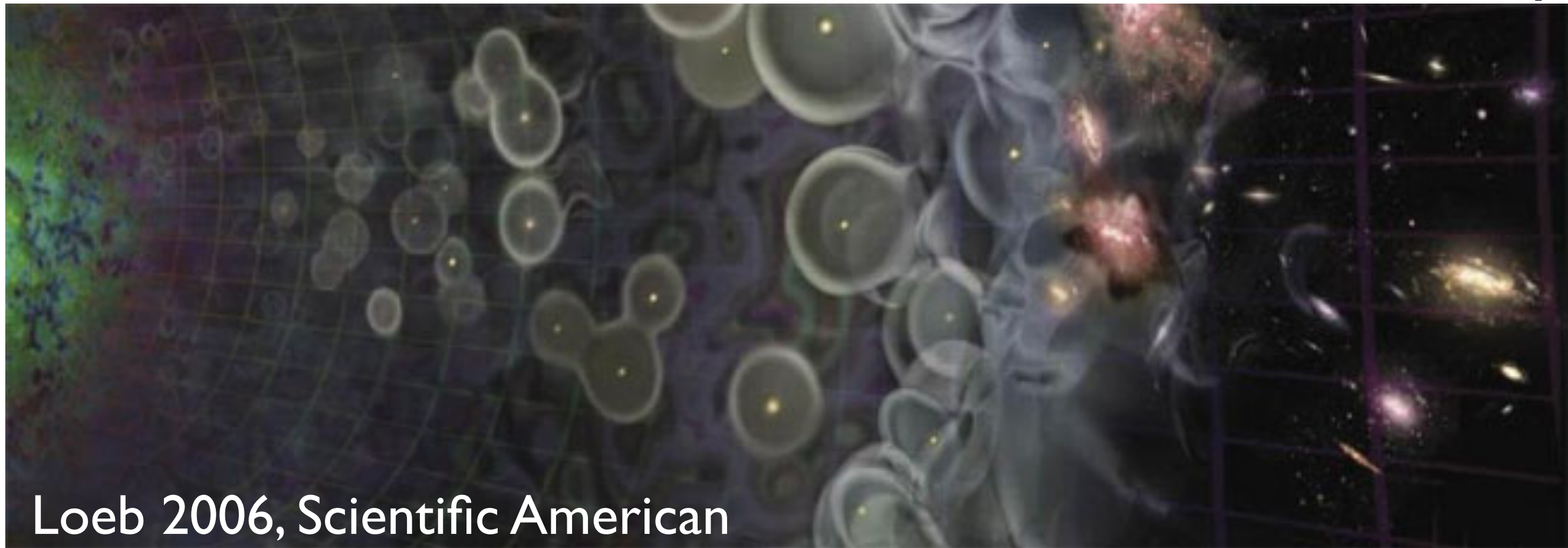


- Powered by black hole  $10^9$  times as massive as the sun
- How do such objects form? How do they grow so rapidly?

# Answers in 21-cm?

CMB

Today

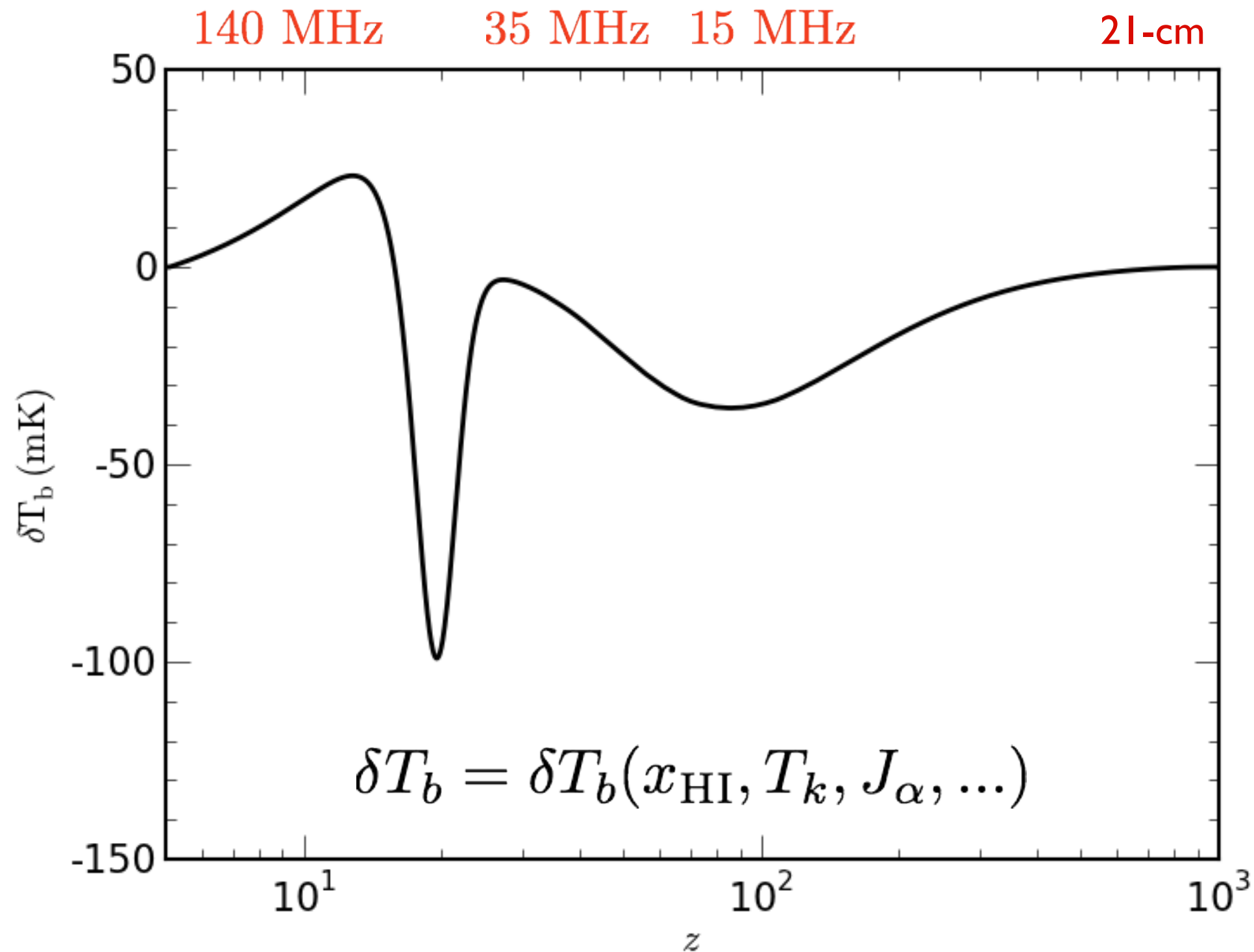


\* Look at space between galaxies instead of galaxies themselves.

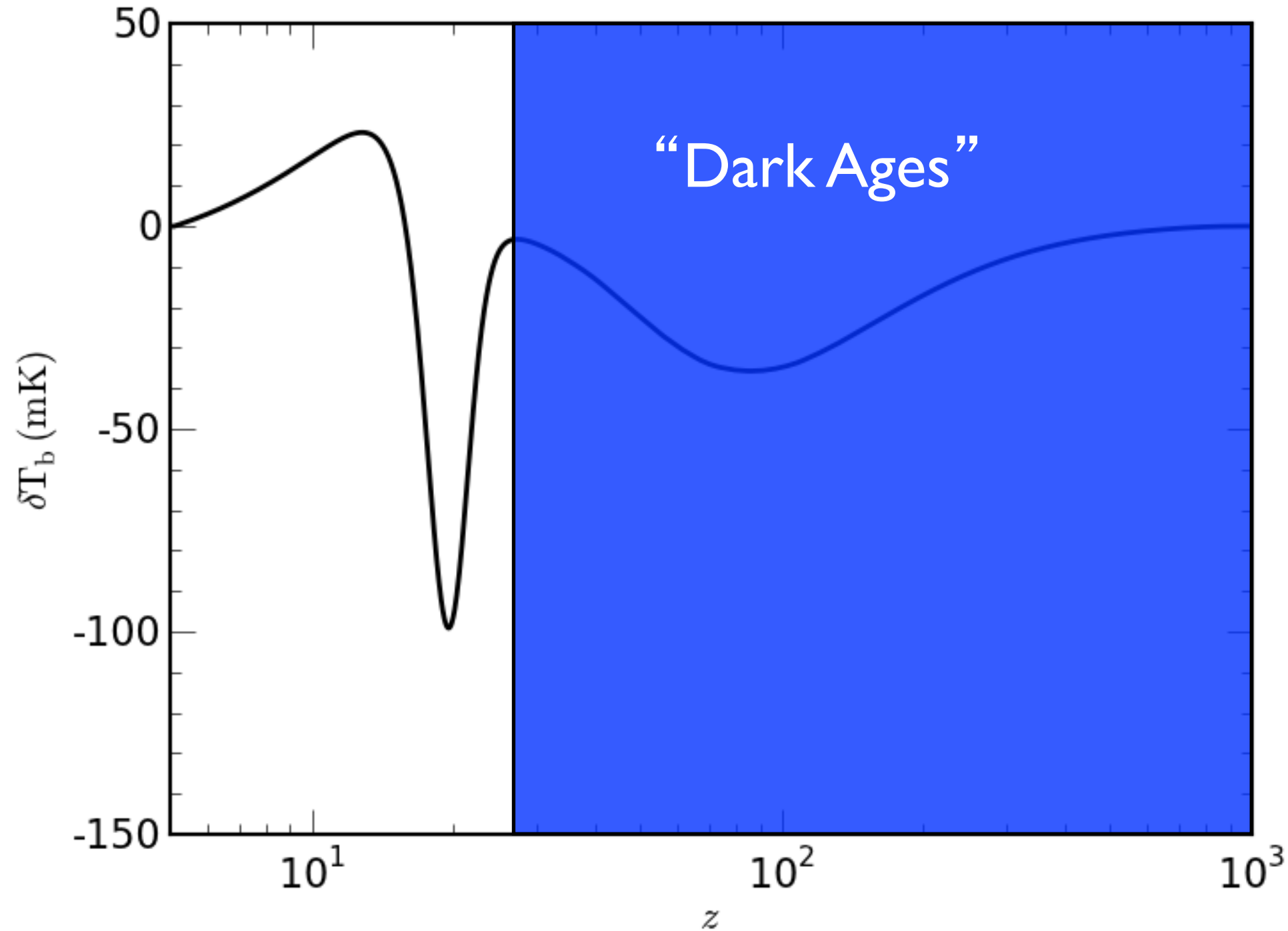


21-cm spin-flip transition

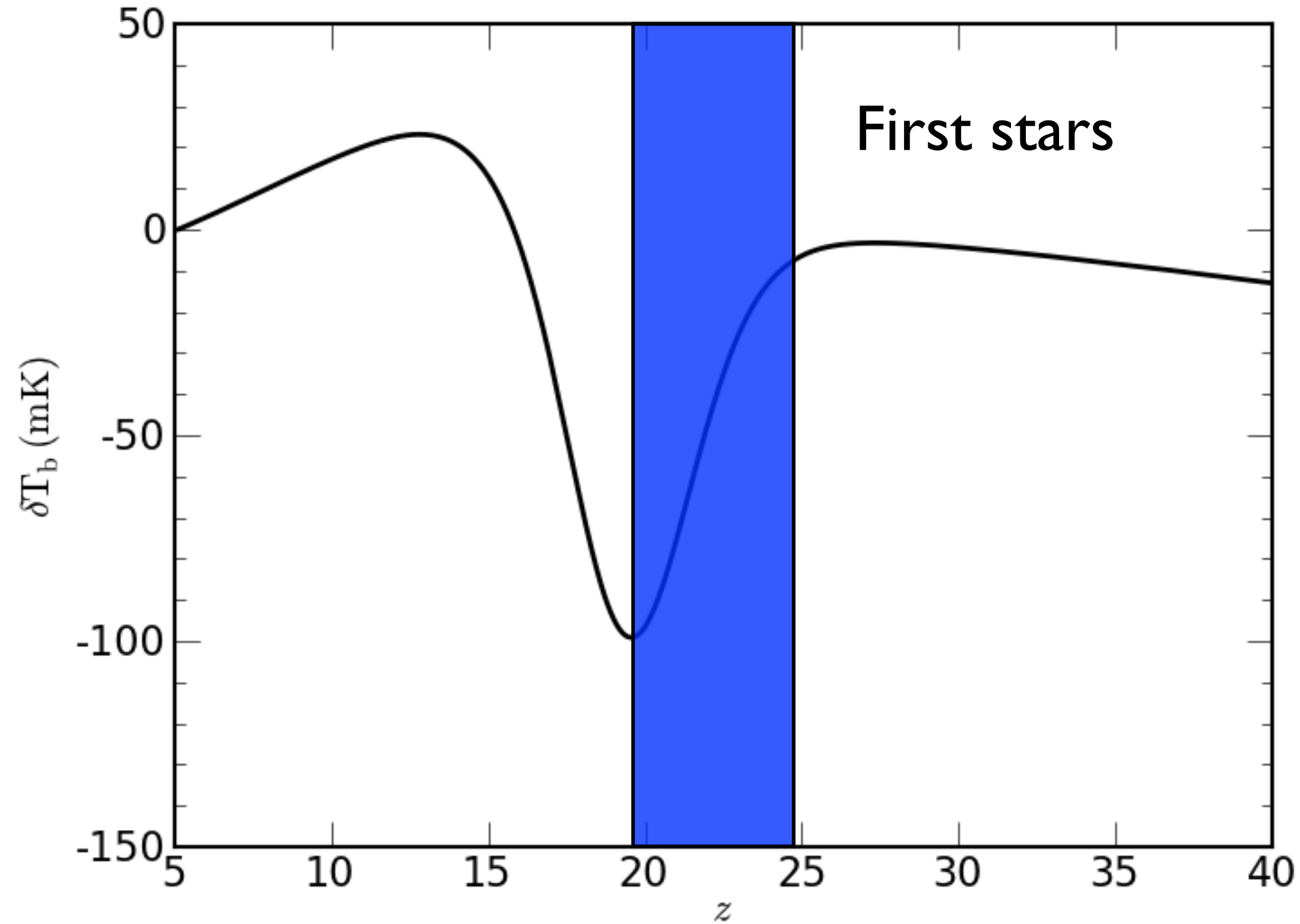
# The Global Signal



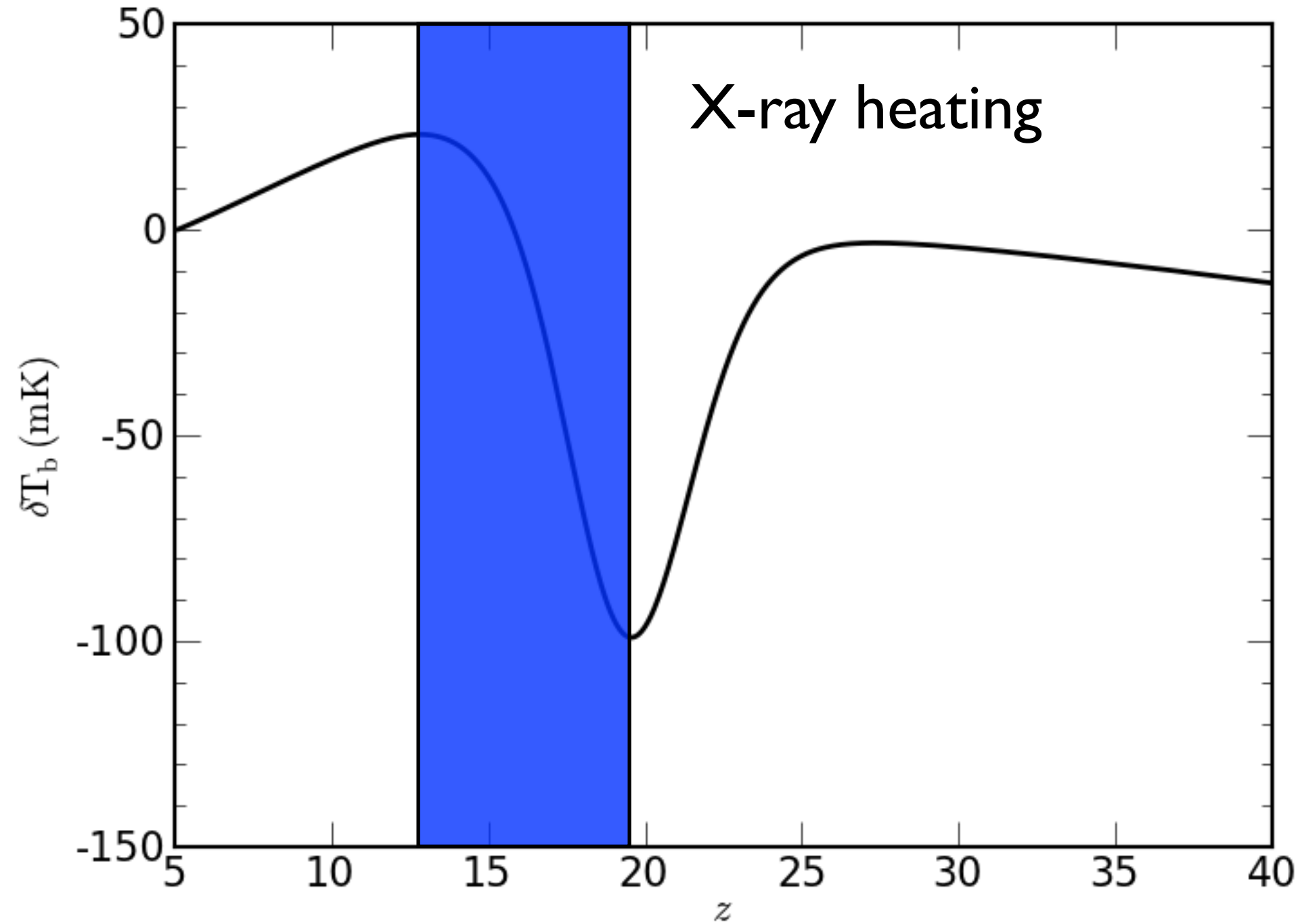
# The Global Signal



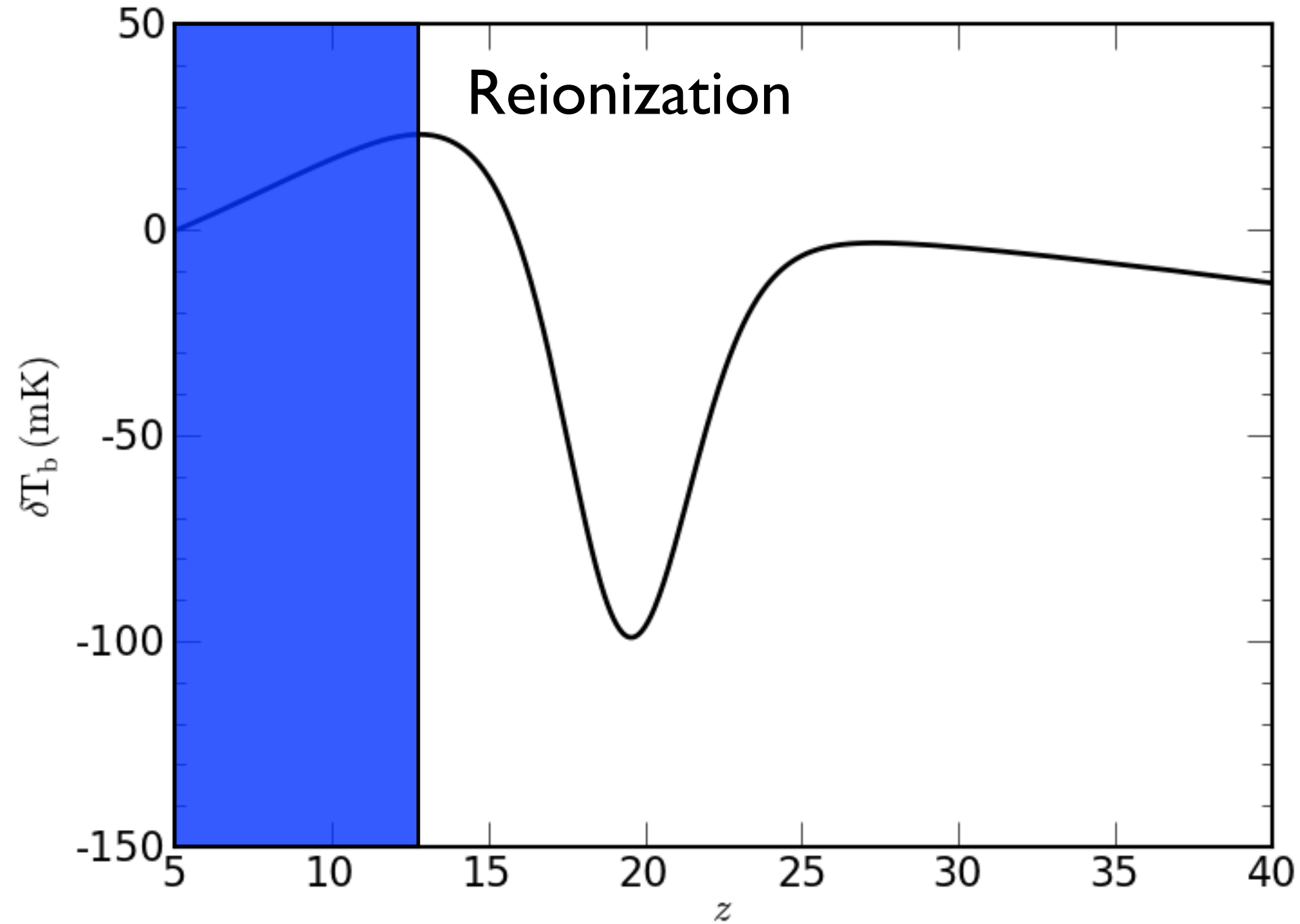
# The Global Signal



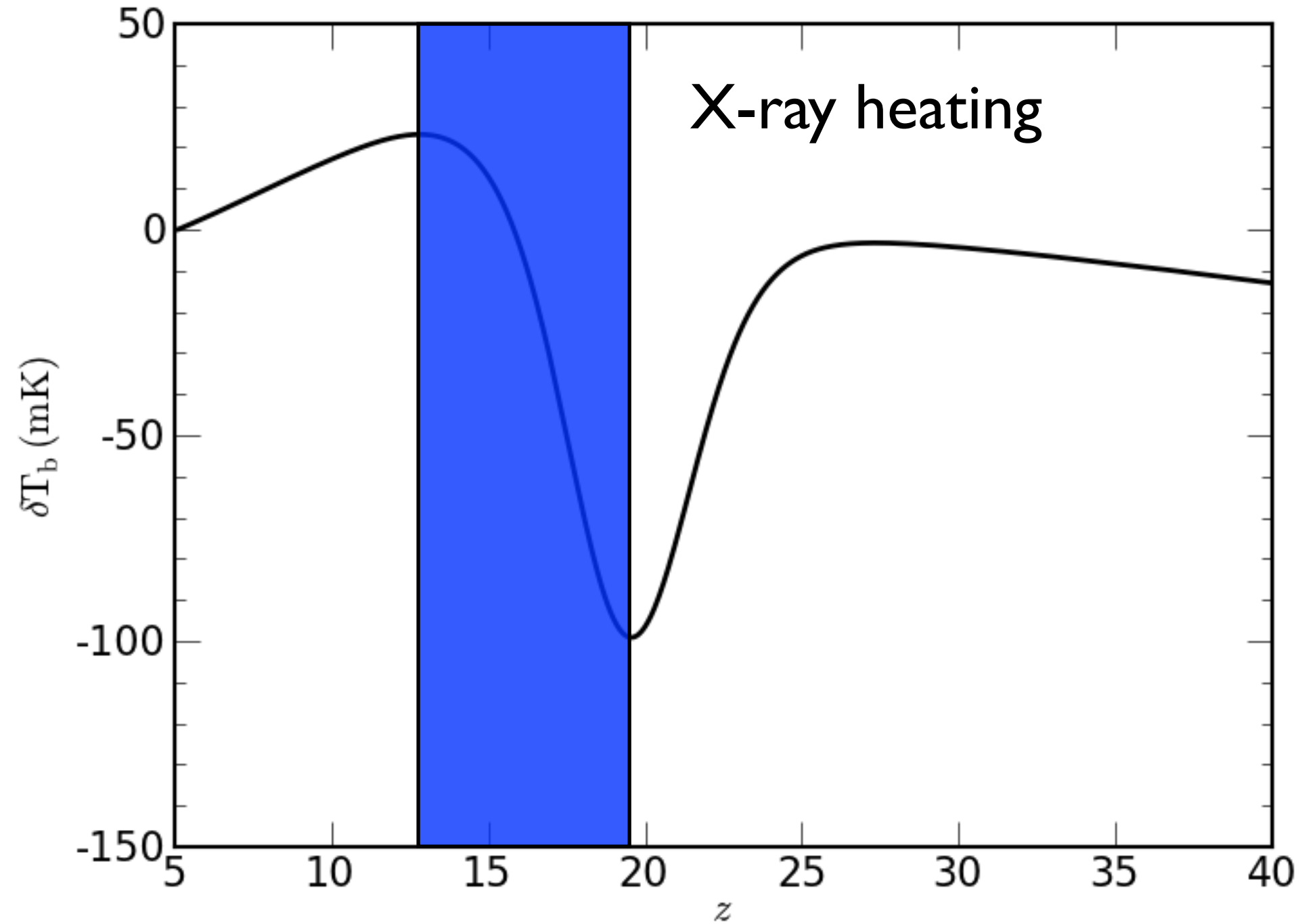
# The Global Signal



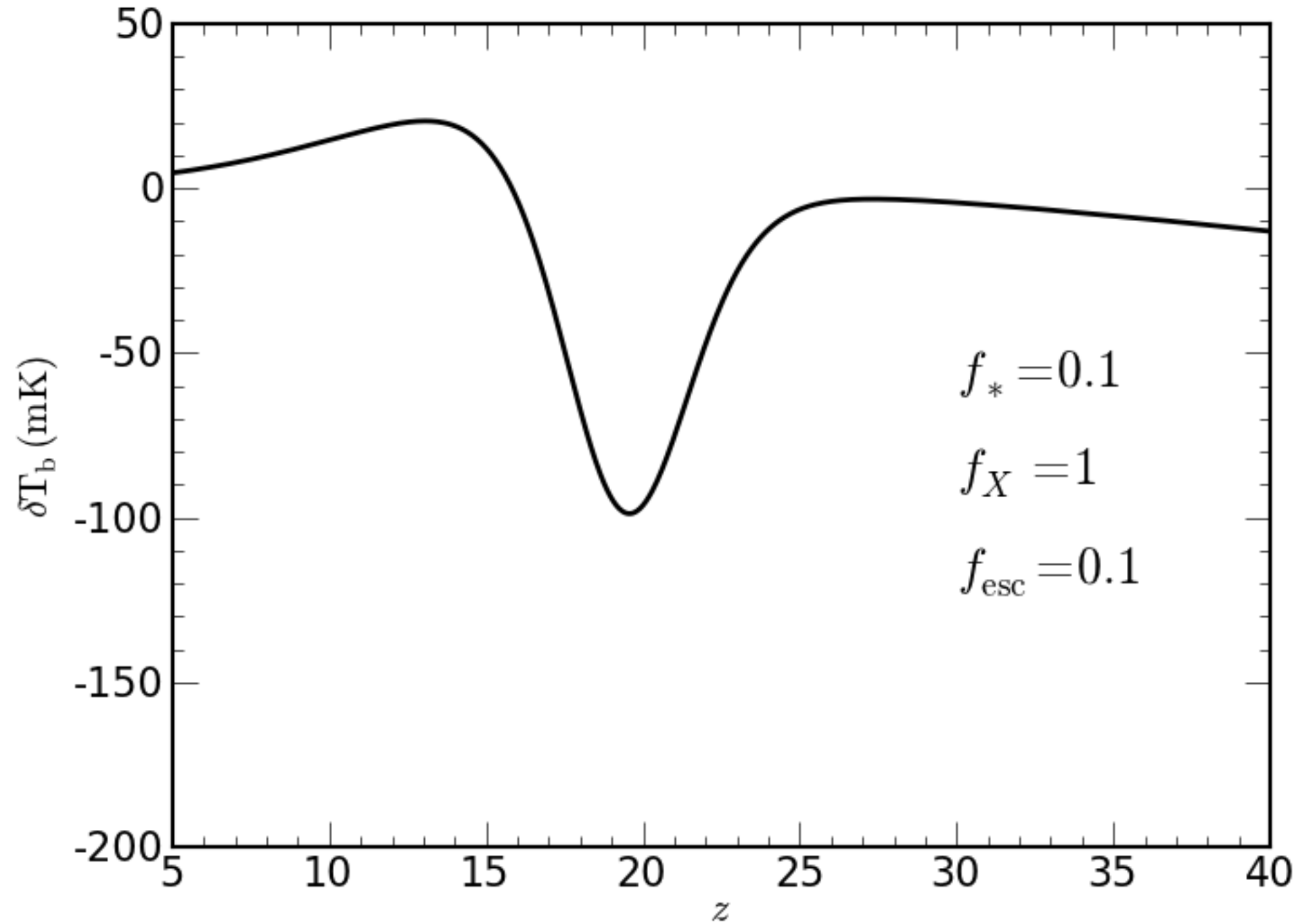
# The Global Signal



# The Global Signal



# The Global Signal



# Magnitude of X-ray heating?

X-ray binaries



$$\frac{2\epsilon_X}{3k_B n_H H(z)} \simeq 1.2 \times 10^4 \text{ K } f_X \left( \frac{f_*}{0.1} \frac{f_{X,h}}{0.2} \right)$$

Furlanetto 2006

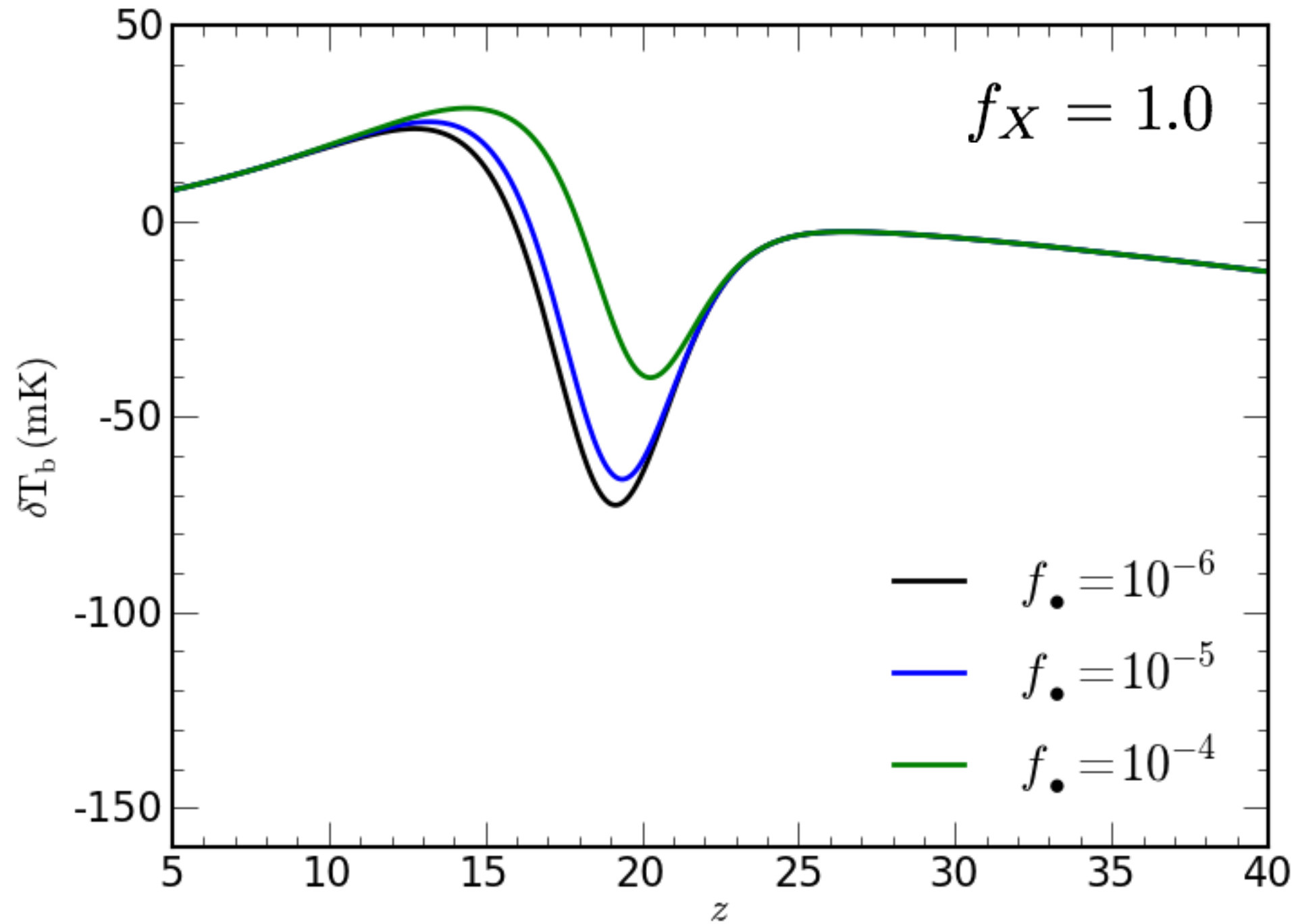
Super-Massive BHs



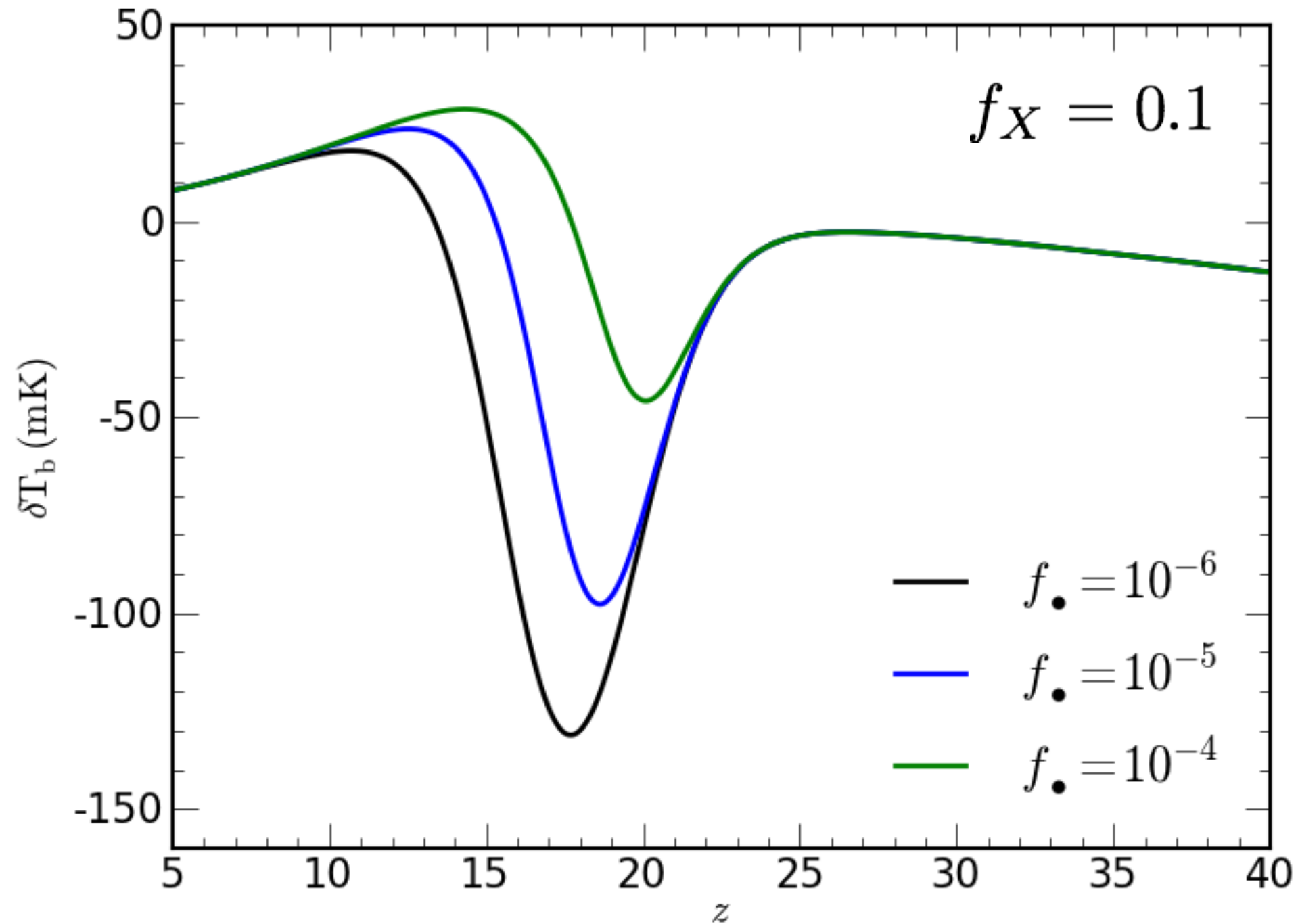
Assume:  $\rho_{\bullet}(z) = f_{\bullet} f_{\text{coll}}(z)$

$$\frac{2\epsilon_{\bullet}}{3k_B n_H H(z)} \simeq 2 \times 10^4 \text{ K } \left( \frac{f_{\bullet}}{10^{-5}} \frac{f_{X,h}}{0.2} \frac{\eta}{0.1} \frac{f_{\text{duty}}}{0.1} \right)$$

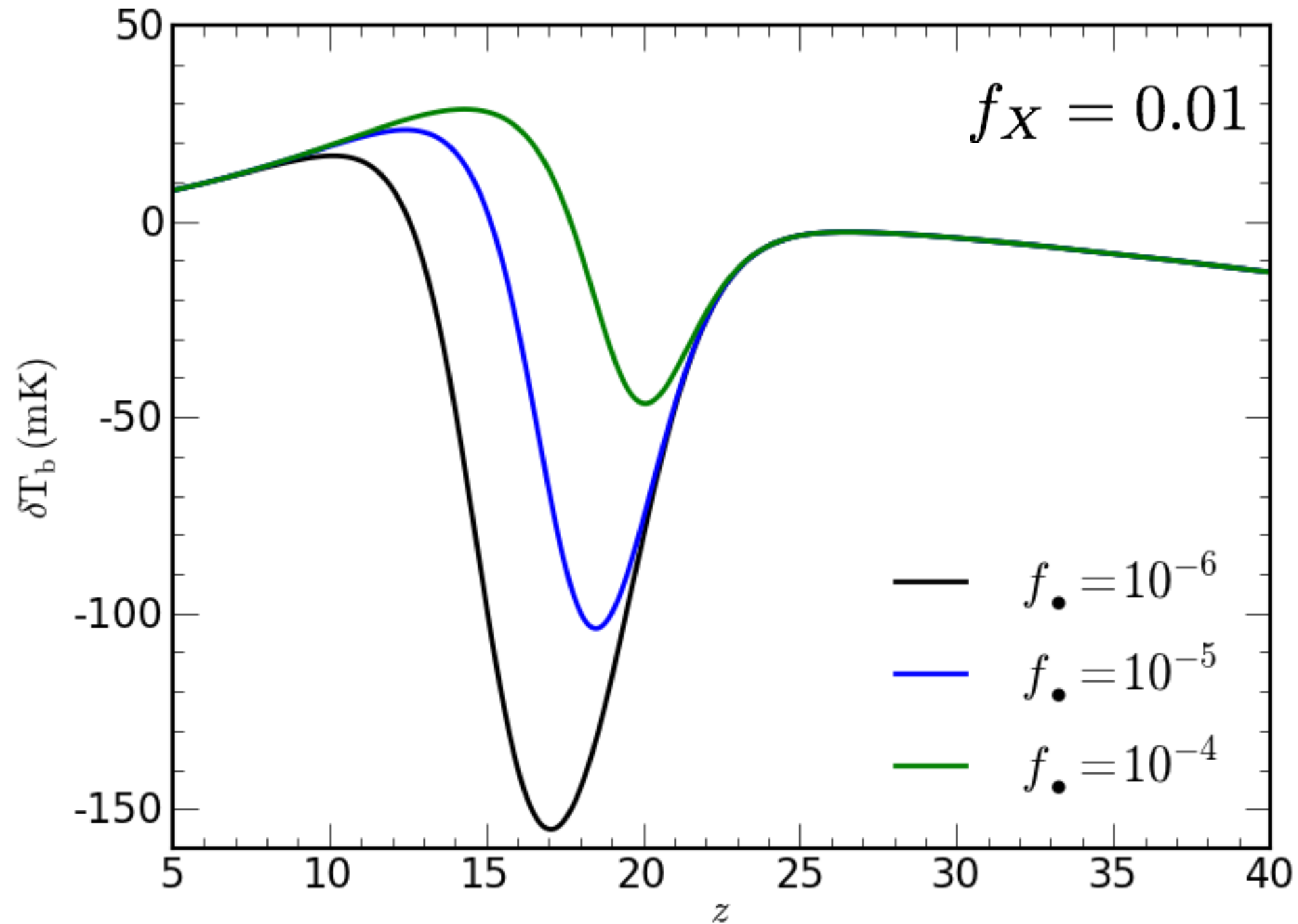
# New SMBH Models



# New SMBH Models

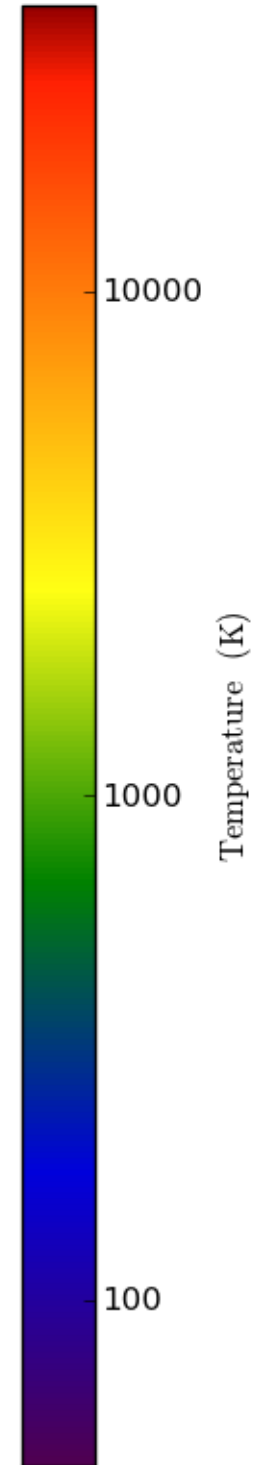
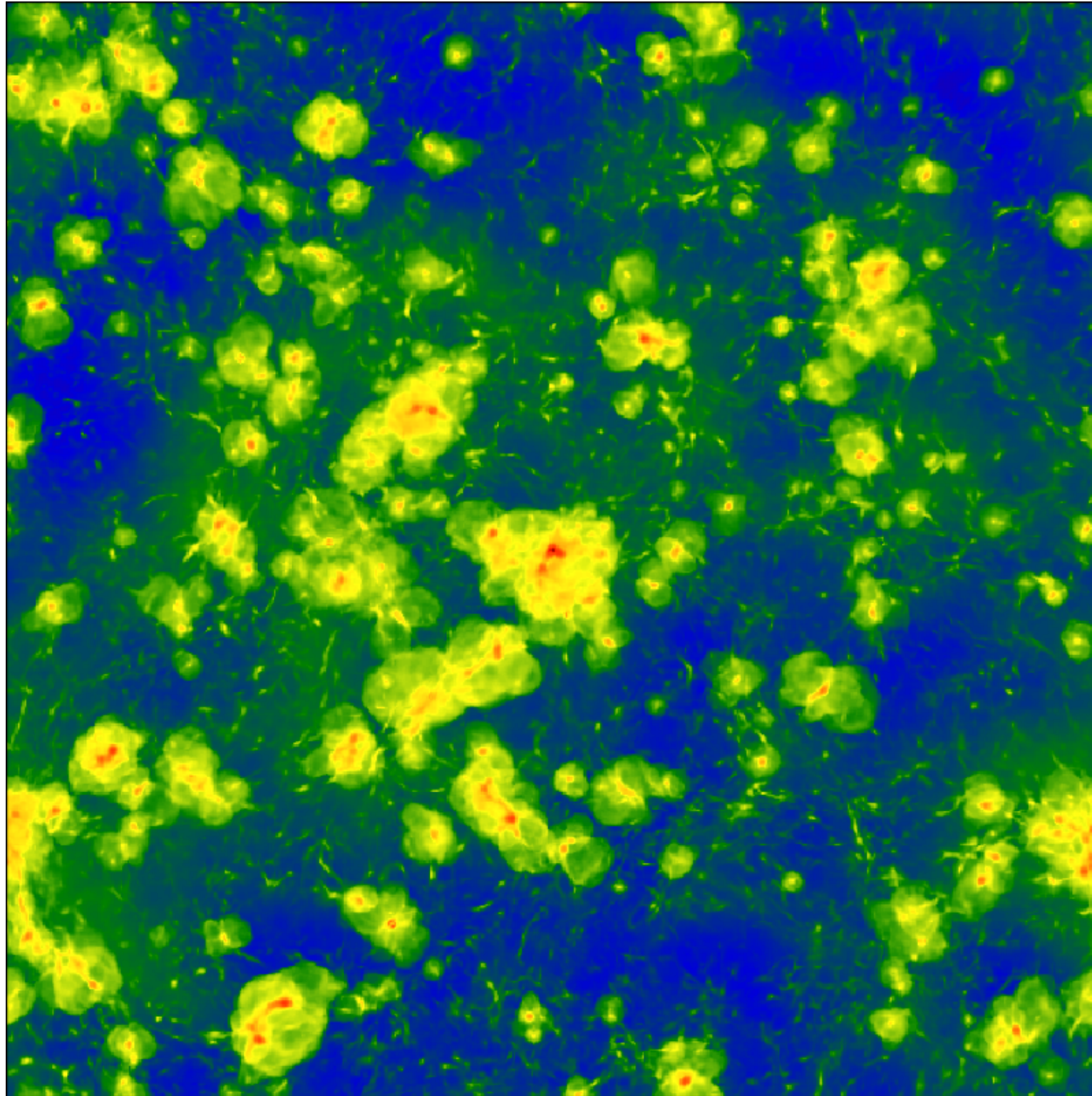


# New SMBH Models



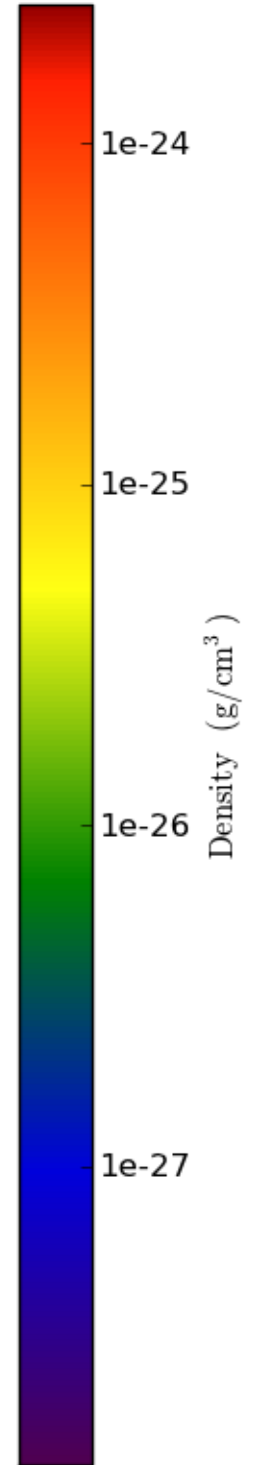
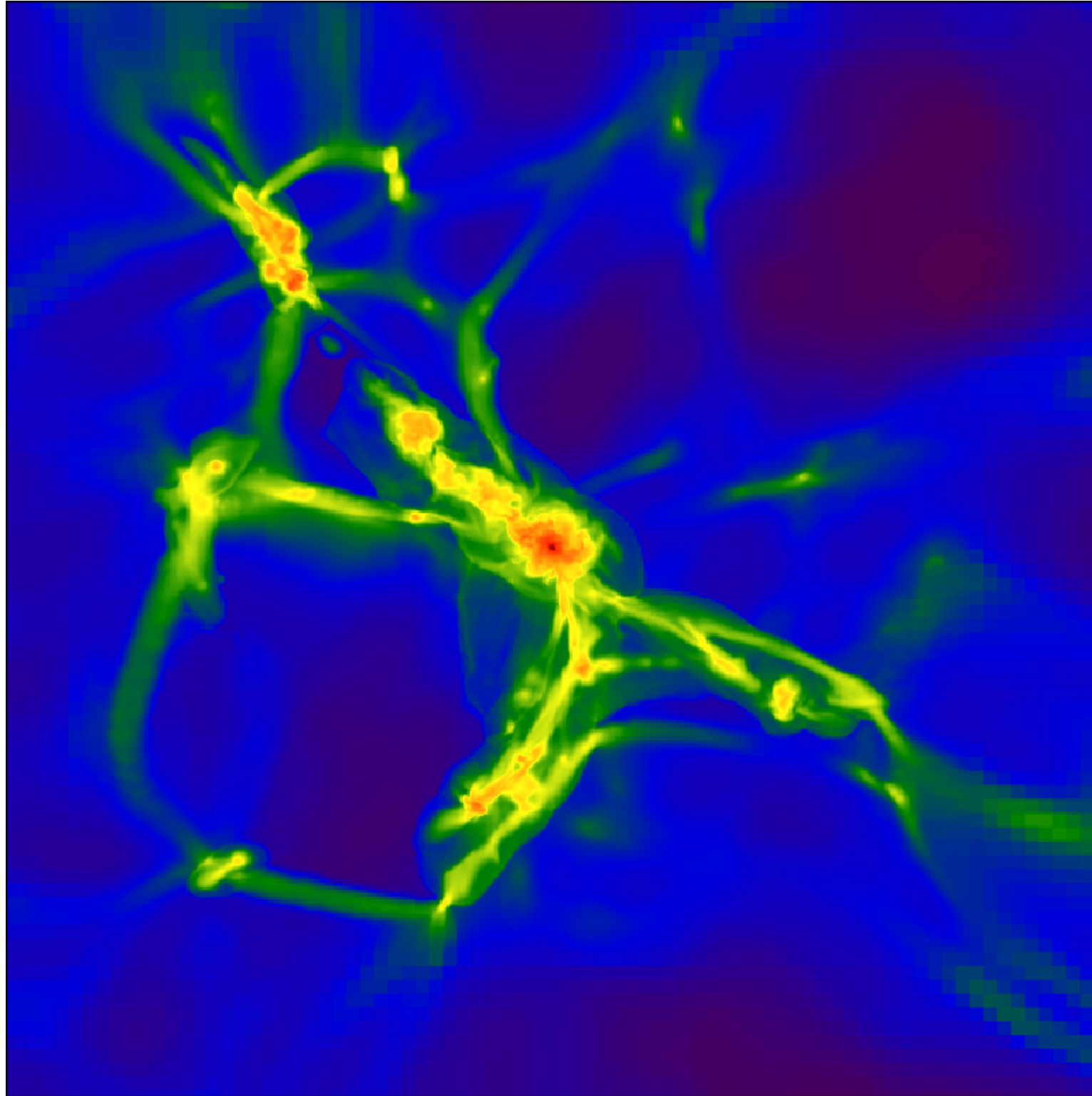
# Ongoing Work

25 Mpc



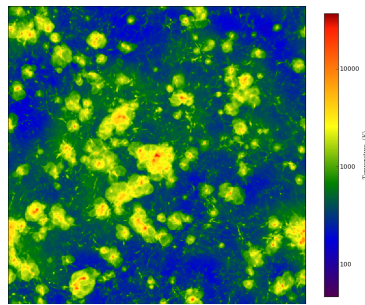
# Ongoing Work

10 kpc

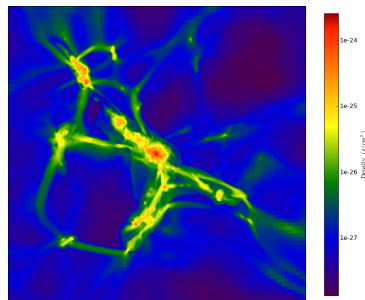


# Summary & Future Work

- X-rays from SMBHs potentially significant for 21-cm, but could be confused:



- Impact of SMBHs in 21-cm fluctuations, analytically & with simulations.



- High-resolution simulations of individual proto-galaxies.

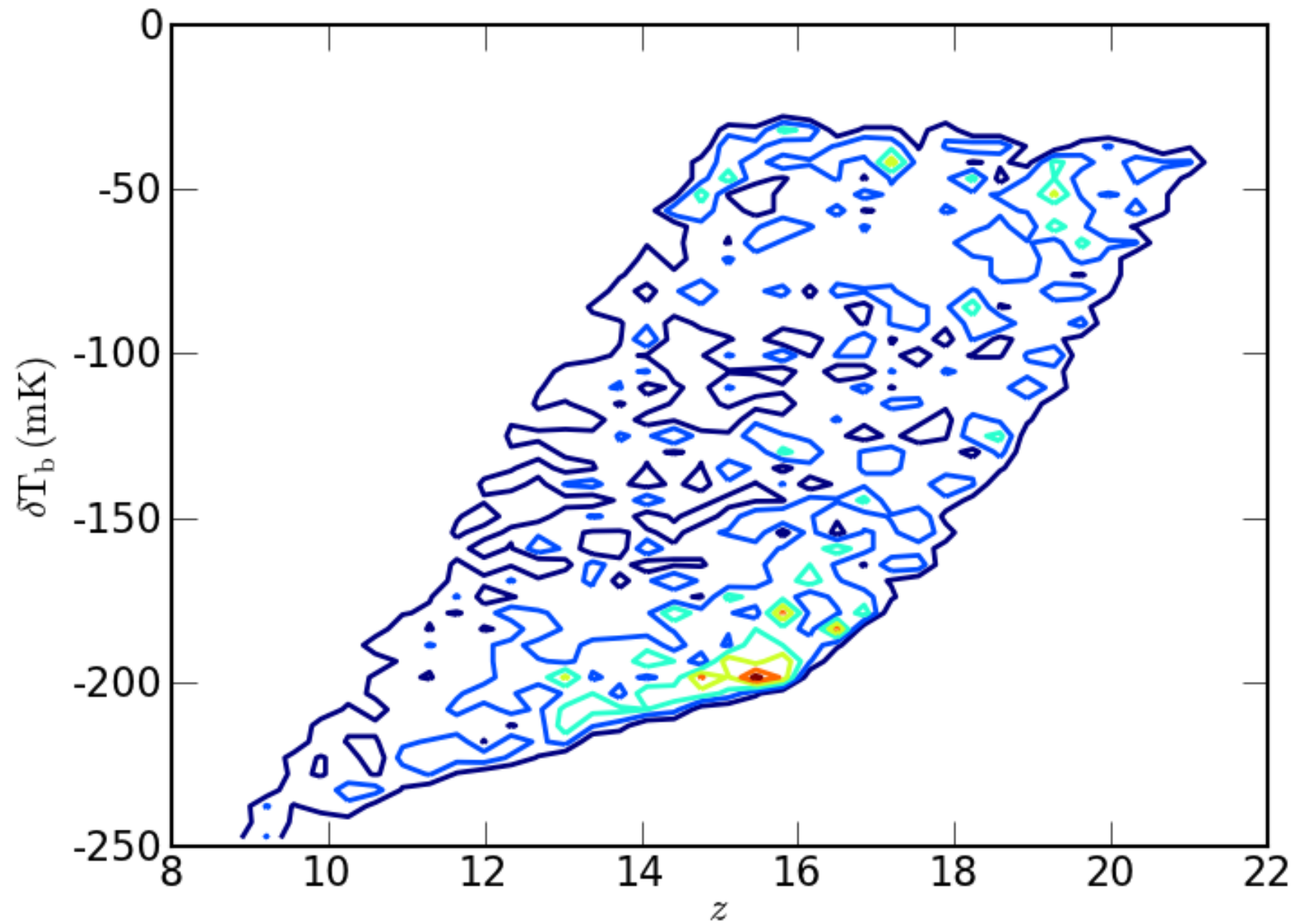
- Use multi-frequency RT algorithm of Mirocha et al. 2012 (arxiv:1204.1944, accepted to ApJ).

A microscopic image showing a dense population of cells. The cells are stained with two different dyes: one that fluoresces in red and another that fluoresces in blue. The red-stained cells are more numerous and appear as bright, glowing clusters. The blue-stained cells are fewer and appear as smaller, less distinct spots. The overall background is dark, making the fluorescent cells stand out.

Questions?



# Turning Point C



$(f_*, f_X, f_{\text{esc}}, f_\alpha, N_{\text{ion}}, T_{\text{vir}})$

$10^5$  models, random parameter values  
spanning range of  $10^3$ - $10^4$

# X-ray Heating

Gilfanov et al. 2003

L58 *M. Gilfanov, H.-J. Grimm and R. Sunyaev*

Ranalli et al. (2003) independently studied X-ray luminosity of normal galaxies using the *ASCA* and *BeppoSAX* archival data and *Chandra* observations of the HDF-N; they found a tight correlation between their X-ray, radio (1.4 GHz) and far-infrared (FIR) fluxes. They suggested that the 2–10 keV luminosity of normal galaxies can be used as an SFR indicator and derived the relation

$$\text{SFR}[M_{\odot} \text{ yr}^{-1}] = \frac{L_{2-10\text{keV}}}{5 \times 10^{39} \text{ erg s}^{-1}}. \quad (2)$$

This formula agrees reasonably well with that obtained by Grimm et al. (2003) for the high-SFR regime [equation (1)]. However, Ranalli et al. (2003) noted that the  $L_X$ -SFR relation was linear in the entire range of the SFRs, including the low-SFR regime, in apparent contradiction to the results of Grimm et al. (2003).

In this Letter, we compare the Grimm et al. (2003) and Ranalli et al. (2003) samples of the galaxies. We demonstrate that the X-ray emission from the low-SFR galaxies in the Ranalli et al. (2003) sample is likely to be 'contaminated' by LMXBs, which are unrelated to current star formation activity. After the 'LMXB contamination' is accounted for, the two data sets agree qualitatively and quantitatively and are consistent with the  $L_X$ -SFR relation expected on the basis of the 'universal' HMXB luminosity function derived by Grimm et al. (2003).

## 2 THE SAMPLES

In the following, we denote Ranalli et al. (2003) and Grimm et al. (2003) samples as R and G, respectively. The data from both samples are plotted together in Fig. 1.

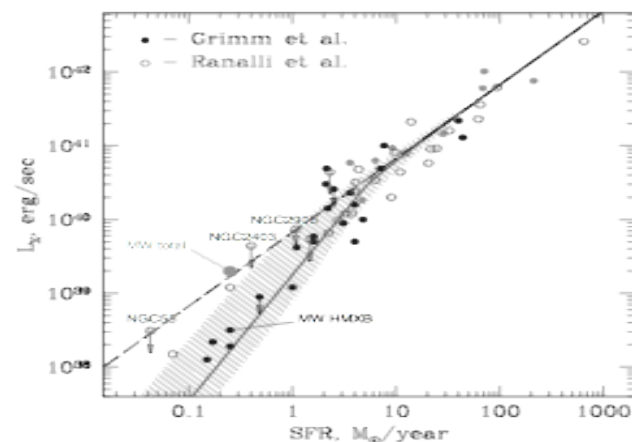


**Figure 1.**  $L_X$ -SFR relation. All points are from Ranalli et al. (2003) and Grimm et al. (2003) are plotted. The galaxies with the expected LMXB fraction exceeding 50 per cent are plotted as upper limits. The thick solid line shows the predicted relation between the most probable values of  $L_X$  and the SFR; the shaded area indicates its 67 per cent intrinsic spread. The straight dashed line shows the expectation mean for  $L_X$ , which would be obtained if X-ray luminosities of many galaxies with similar SFR were averaged. To demonstrate the importance of the LMXB contribution at low SFR/ $M_*$ , both HMXB and total luminosities are plotted for the Milky Way. This figure is available in colour in the online version of the journal on *Synergy*.

## 2.1 The local galaxies

The two samples, although differently constructed, overlap substantially, with nine galaxies (out of 23 in each sample) present in both. Sample R was derived using a more rigorously defined construction algorithm. In almost all cases, the authors adopted different distances and different values of the SFR. Grimm et al. (2003) derived SFR values by averaging the results of several independent estimators based on UV, FIR,  $H_{\alpha}$  and radio flux measurements, whereas Ranalli et al. (2003) used radio flux measurements. The X-ray fluxes were obtained from different observations, sometimes by different instruments and are obviously affected by variability of the X-ray emission from the galaxies. For some of the galaxies, the X-ray luminosity was calculated by Grimm et al. (2003) as a direct sum of the luminosities of compact sources detected by *Chandra*.

Fig. 2 compares positions of the galaxies present in the both samples in the  $L_X$ -SFR plane. Note that the difference in the adopted distances does not have an effect at high values of SFR where the  $L_X$ -SFR relation is linear, but it might destroy the correlation in the non-linear low-SFR regime.

## 2.2 Hubble Deep Field North

Both Grimm et al. (2003) and Ranalli et al. (2003) used similar selection criteria. Each sample contains seven sources, of which six are present in both samples. Sources #185 and #148 (according to table 2 in Brandt et al. 2001) are absent from the R and G samples, respectively. The latter was excluded from sample G because no 1.4-GHz flux was detected, with the upper limit of 23  $\mu\text{Jy}$  (Richards et al. 1998). The main difference lies in computing the X-ray fluxes and luminosities. Grimm et al. (2003) used 2–8 keV fluxes from the *Chandra* catalogue and  $K$ -corrected them to a 2–10 keV

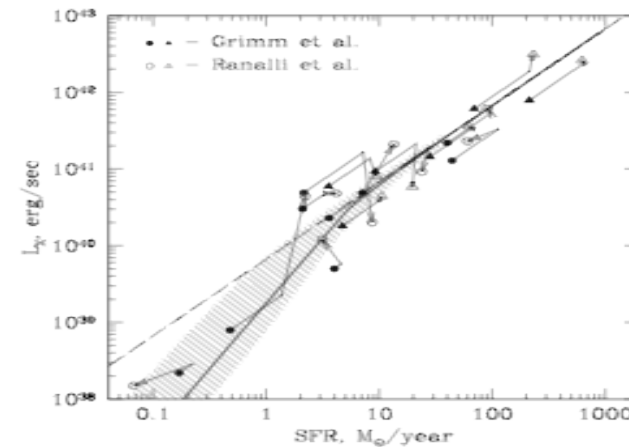


**Figure 2.** Comparison of the data for local (circles) and HDF-N (triangles) galaxies present both in Grimm et al. (2003) and Ranalli et al. (2003) samples. For each galaxy, its positions in two samples are connected by a broken line, with the arrow directed from G to R. The first segment of each broken line shows the effect of the difference in the source distance or cosmological parameters; the second segment shows the cumulative effect of other factors, such as variability and difference in the SFR values. This figure is available in colour in the online version of the journal on *Synergy*.

Local Universe:

$$\left( \frac{L_X}{\text{erg s}^{-1}} \right) \propto f_X \left( \frac{\text{SFR}}{M_{\odot} \text{ yr}^{-1}} \right)$$

$L_X$  dominated by X-ray binaries

